Title:

A simple approach to forest structure classification using airborne laser scanning that can be

adopted across bioregions

Authors:

Syed Adnan*(1)(2)(3), Matti Maltamo (1), David A. Coomes (2), Antonio García-Abril (4),

Yadvinder Malhi (5), José Antonio Manzanera (4), Nathalie Butt (6)(5), Mike Morecroft (7), Rubén

Valbuena*(2)

Affiliations:

(1) University of Eastern Finland, Faculty of Forest Sciences. PO Box 111. FI-80101. Joensuu,

Finland. adnan@uef.fi; matti.maltamo@uef.fi.

(2) University of Cambridge, Department of Plant Sciences. Forest Ecology and Conservation.

Downing Street, CB2 3EA Cambridge, UK. dac18@cam.ac.uk; rv314@cam.ac.uk

(3) National University of Sciences and Technology, Institute of Geographical Information

Systems, 44000 Islamabad, Pakistan.

(4) Universidad Politecnica de Madrid, College of Forestry and Natural Environment, Research

Group SILVANET, Ciudad Universitaria, 28040 Madrid, Spain.

antonio.garcia.abril@upm.es; joseantonio.manzanera@upm.es.

(5) University of Oxford, School of Geography and the Environment. Environmental Change

Institute. OX1 3QY Oxford, UK. yadvinder.malhi@ouce.ox.ac.uk.

(6) The University of Queensland, School of Biological Sciences, St. Lucia, Queensland, 4072,

Australia. n.butt@uq.edu.au.

(7) Natural England. Cromwell House. 15 Andover Road. SO23 7BT, Winchester, UK.

mike.morecroft@naturalengland.org.uk.

*Corresponding authors.

Highlights

- A simple two-tier approach to classify forest structural types (FSTs)
- Higher tier classifies single storey / multi-layered / reversed J
- A lower tier classifies young/mature and dense/sparse subtypes
- Airborne laser scanning was employed for a multisite FST classification
- This approach paves the way toward transnational assessments of FSTs

Abstract

Reliable assessment of forest structural types (FSTs) aids sustainable forest management. We developed a methodology for the identification of FSTs using airborne laser scanning (ALS), and demonstrate its generality by applying it to forests from Boreal, Mediterranean and Atlantic biogeographical regions. First, hierarchal clustering analysis (HCA) was applied and clusters (FSTs) were determined in coniferous and deciduous forests using four forest structural variables obtained from forest inventory data – quadratic mean diameter (QMD), Gini coefficient (GC), basal area larger than mean ($BALM$) and density of stems (N) –. Then, classification and regression tree analysis (CART) were used to extract the empirical threshold values for discriminating those clusters. Based on the classification trees, GC and $BALM$ were the most important variables in the identification of FSTs. Lower, medium and high values of GC and $BALM$ characterize single storey FSTs, multi-layered FSTs and exponentially decreasing size distributions (reversed J), respectively. Within each of these main FST groups, we also identified young/mature and sparse/dense subtypes using QMD and N. Then we used similar structural predictors derived from ALS – maximum height (Max), L-coefficient of variation (Lcv), L-skewness ($Lskew$), and percentage of penetration ($cover$), – and a nearest neighbour method to predict the FSTs. We obtained a greater overall accuracy in deciduous forest (0.87) as compared to the coniferous forest (0.72). Our methodology proves the usefulness of ALS data for structural heterogeneity assessment of forests across biogeographical regions. Our simple two-tier approach to FST classification paves the way toward transnational assessments of forest structure across bioregions.

1. Introduction

The structural complexity of forest affects the growth rate of individual trees and the dynamics of tree communities (Donato et al., 2012). Knowledge of this structural variations is key to understand ecosystem functioning (Coomes and Allen, 2007a) and sustainable forest management planning (Bergeron et al., 2002). Accurate structural heterogeneity assessment and stand development categorization is important for long-term prediction of biomass production (Gove, 2004; Bourdier et al., 2016) and turnover (Marvin, 2014), biodiversity (Gove et al., 1995; Pommerening, 2002), and for identifying important habitats for wildlife (Vihervaara et al., 2015). It can also assist the planning and monitoring of different silvicultural regimes and forest management strategies (McElhinny et al., 2005; Valbuena et al., 2016a). Forest structure information may also be helpful to reduce sampling efforts and costs (Maltamo et al., 2010; Moss, 2012).

From an ecological point of view, forest structure is an important attribute at community level and consists of three major components: horizontal structure (spatial pattern, gaps and tree groups), vertical structure (number of tree layers) and species richness (O'Hara et al., 1996; Zimble et al., 2003; Pascual et al., 2008). However, unlike other forest attributes, forest structure lacks a clear and fixed definition, which thus varies from one application to another (Maltamo et al., 2005). Various approaches are found in the literature for identifying forest structural types (FSTs), such as stand developments classes (Valbuena et al., 2016a), patterns of growth and mortality (Coomes and Allen, 2007b), ecology of tree populations (O'Hara et al., 1996), stand age (O'Hara and Gersonde, 2004) or tree diameter distributions (Linder et al., 1997). There is also no consensus on the relevant classes to identify as FSTs, and thus a disparate number of them can be found, for example including understorey vegetation/regeneration (Gougeon et al., 2001), single storey to multi-storey structures (Zimble et al., 2003; O'Hara and Gersonde, 2004; Maltamo et al., 2005), suppressed tree storey (Hyyppä et al., 2008), young and mature stands (Means et al., 2000; Næsset, 2002), sparse and dense stands (Maltamo et al., 2004; Hyyppä et al., 2008) and reversed J-types of forest structures (Linder et

98 al., 1997; Valbuena et al., 2013). There is also great disparity on the forest variables and indicators

99 employed for quantitative assessment of structural heterogeneity (Lexerod and Eid, 2006; Valbuena

100 et al., 2014) and FST categorization (Valbuena et al., 2013). Overall, FST definition and description

101 may be dependent on the observer and thus there is a need to develop more objective quantitative

102 approaches (e.g., Moss 2012; Valbuena et al., 2013) that can be useful across biomes and bioregions.

103 Here we propose a region-independent FST characterization by a combination of attributes describing

104 tree diameter distribution – location, spread, skewness and density – using the following forest

105 structural attributes: quadratic mean diameter (QMD), Gini coefficient (GC), basal area larger than

106 mean ($BALM$) and density of stems (N).

107 The most common descriptors used to categorize forest dynamics and development are the QMD and

108 N (Gove, 2004). The QMD can be described as the diameter of a tree having an average basal area

109 and N is the number of stems per hectare (Curtis, 1982). These two parameters (QMD and N) are key

110 to determine the need for planting or thinning in forest stands. Combinations of QMD and N are

111 typically employed in the determination of forest development classes (e.g., Valbuena et al., 2016a),

112 maximum stand density limits and occurrences of mortality in forest stands, impacts of habitat

113 fragmentation on forest structure (Echeverría et al., 2007) and development of stand density diagrams

114 (Newton, 1997; Gove, 2004).

115 The GC, an index of inequality widely used in econometrics has become popular in forest science due

116 to its robust statistical properties and capacity to rank FSTs based on tree size variability (Lexerød

117 and Eid, 2006; Duduman, 2011; Valbuena et al., 2012). It has been used to evaluate size inequality

118 (Weiner, 1985), structural heterogeneity (Lexerød and Eid, 2006), successional stages (Duduman,

119 2011; Valbuena et al., 2013), relationship of relative dominance in forest stands (Valbuena et al.,

120 2012) and to discriminate among differently-shaped diameter distributions (Bollandsås and Næsset,

121 2007; Valbuena et al., 2016a). Valbuena (2015) postulated that values of GC and $BALM$ describe the

spread and skewness of the tree size distribution, respectively, and that together they provide the best means of categorising FSTs (Gove, 2004; Valbuena et al., 2014). These FSTs can be analysed further to indicate whether trees interaction are dominated by symmetric competition associated with resource depletion, or asymmetric competition associated with resource pre-emption (Weiner, 1985). Although some theoretical values have been postulated discriminating FSTs from GC and $BALM$ (Valbuena et al., 2013, 2014), there is a need to empirically investigate threshold values of GC and $BALM$ in such categorization.

Airborne laser scanning provides an excellent means for forest structural heterogeneity assessment as the ALS data produce accurate canopy information (Maltamo et al., 2005; Valbuena et al., 2016b). Metrics derived from ALS height distribution describe the key characteristics of forest structure and could be used to monitor various aspects of forest dynamics (Jaskierniak et al., 2011; Valbuena et al., 2013). Numerous studies have used ALS data and demonstrated that it is a useful tool to characterize variation in forest structure (Maltamo et al., 2005; Pascual et al., 2008; Valbuena et al., 2017; Fedrigo et al., 2018). For this reason, it is important to find methodologies for prediction of FSTs from ALS which can be robust across ecoregions.

The objective of this research was to carry out a classification of FSTs using a combination of these four forest attributes – QMD, GC, $BALM$ and N– postulating that together they can achieve a full description for forest structure where each FST contains a range of all possible horizontal and vertical structures. Using data from three different biogeographical regions –Boreal, Mediterranean and Atlantic–, we aimed at developing a region-independent methodology for FST characterization. We also evaluated the capacity of using ALS to achieve a reliable classification of those FSTs.

2. Material and Methods

2.1. Study Sites and Data Collection

145   Forest and ALS data from three biogeographical regions (**Figure 1**) were used to identify, classify

146   and predict FSTs:

147   *a) Boreal: Kiihtelysvaara Forest, Finland*

148   Kiihtelysvaara forest is a common boreal managed forest located in the Eastern Finland (62˚ 31′ N,

149   30˚ 10′ E). The area is dominated by Scots pine with the presence of Norway spruce and deciduous

150   species as minor tree species. The field data consisted of 79 squared plots collected during May-June

151   2010 (Maltamo et al., 2012). Plot size was 20×20 m, after some of them were subsampled from larger

152   plots (Valbuena et al., 2014) with the intention to analyse a homogeneous dataset consistent with the

153   other two regional sites involved in this study. The data included diameters and breast height (dbh)

154   for all trees with a height greater than 4 m or $dbh > 5\ cm$. A high resolution ALS dataset was

155   acquired on June 26, 2009 using ATM Gemini sensor (Optech, Canada), Its scan density 11.9

156   pulses·m^{-2} obtained from 600-700 m above ground level at a pulse rate of 125 kHz. Field of view

157   (FOV) was 26˚ and scan swath was 320 m wide with a 55% side overlap between the strips.

158   *b) Mediterranean: Valsaín Forest, Spain*

159   Valsain forest is a shelterwood managed (Valbuena et al., 2013) Scots pine area located in Segovia

160   province, Spain (40°48′ N 4°01′ W), at 300-1,500 m above sea level. The field data consisted of 37

161   circular plots with 20 m radius measured during summer 2006. All seedlings and saplings were

162   measured within an inner 10 m radius subplot, whereas in the outer annulus only trees with $dbh >$

163   10 cm were measured. ALS data were captured on September 2006 using an ALS50-II from 1,500

164   m above ground level with a pulse rate of 55 kHz from Leica Geosystems (Switzerland). A FOV of

165   25° rendered a 665 m ground bidirectional scan width with 40% side lap. The average scan density

166   of ALS data was 1.15 pulses·m^{-2}.

167   *c) Atlantic: Wytham Woods, United Kingdom*

168 Wytham Woods is a managed lowland ancient woodland located in Oxfordshire, UK (51°46' N, 1°20'

169 W). The dominant species are ash, sycamore as well as oak, hazel and maple trees (Savill et al., 2011).

170 We used data from a permanent plot with a total area of 18 ha measured in 2010. The area of the

171 permanent plot is further subdivided into 450 subplots sizing 20×20 m each. Field data included dbh

172 of all stems greater than 1 cm. Leica ALS50-II LiDAR system with a 96.8 kHz pulse rate and 35˚

173 FOV was used from 2,500 m above sea level for ALS data acquisition and a low resolution ALS data

174 of 0.918 pulses·m^{-2} density were acquired on June 24, 2014. Since growth is low in ancient woodlands

175 and FST dynamics change slowly, the time differences between field and remote sensing acquisition

176 can be assumed to have little effect in the classifications.

177 *** *approximate position of Figure 1* ***

178 *2.2. Data Analyses*

179 Forest stand attributes and characteristics were calculated by aggregating the tree-level information

180 into per-hectare totals at plot-level (**Table 1**): we calculated quadratic mean diameter (QMD, cm), the

181 Gini coefficient (GC) (Weiner, 1985), the proportion of basal area larger than the QMD ($BALM$)

182 (Gove, 2004), and stem density (N, stems·ha^{-1}). The first task was to identify the potential clusters

183 that could be rendered when using these four descriptors ($QMD, GC, BALM$ and N). We grouped the

184 data into coniferous (Boreal plus Mediterranean combined) and deciduous forests (Atlantic), after

185 preliminary results showed that it was more convenient to carry out separate analyses for these two

186 groups. The total number of field plots in the coniferous group was 116, and thus we randomly

187 subsampled 116 out of 450 field plots from the deciduous group, to make further analysis consistent

188 and obtain directly comparable results. Then, we applied hierarchical clustering analysis (HCA) to

189 both coniferous and deciduous forest to optimize the clusters that can be rendered from the chosen

190 forest attributes. The second task was to find the threshold values in both coniferous and deciduous

191 forests which, when applied to $QMD, GC, BALM$ and N, were best able to determine FSTs. This task

192   was carried out using classification and regression trees (CART), which in this case were employed

193   to classify the forest data into the clusters identified by the HCA analysis. The last task was to

194   investigate the reliability of the FST classification obtained from ALS. The ALS classification was

195   carried out using nearest neighbor (kNN) imputation method. The FSTs identified as a result of the

196   HCA were employed as response variable in the kNN. All analyses were carried out using the R

197   environment (R Core Team, 2018).

198   *** approximate position of Table 1 ***

199   *2.2.1. Hierarchical Clustering Analysis*

200   HCA consists of a series of successive merging (agglomerative method) or splitting (divisive method)

201   steps of individual observations based on proximity measures (similarity, dissimilarity or distance)

202   and is used to determine meaningful clusters in a large group of data. We calculated the most widely

203   used proximity measure, which is the Euclidian distance:

204   $$d_{kl} = \sqrt{\sum_{m=1}^{p}(X_{km} - X_{lm})^2}, \tag{1}$$

205   where, d_{kl} is the Euclidian distance between two individual cases k and l in a m-dimensional space

206   (of $m = 1,2 \ldots p$ variables), and X_{km} and X_{lm} are their values of the mth variable. Since

207   $QMD, GC, BALM$ and N were measured in different units, calculating the proximity measure d_{kl}

208   directly on their original scales would unfairly weight some variables over others. To deal with this

209   contingency, we applied a standardization of the raw variables prior to Euclidian distance calculation.

210   We chose a range-equalization method. Thus, each variable value X was normalized to a scale 0 to 1,

211   according to their empirical minimum (X_{min}) and maximum (X_{max}) values (**Table 1**):

212   $$Z = (X - X_{min})/(X_{max} - X_{min}), \tag{2}$$

213 Then, one of the most challenging stages in clustering analysis is the need to determine an optimal

214 number c of clusters because the HCA may run until a single cluster containing all observations

215 (agglomerative method) or c number of clusters each containing one observation (divisive method)

216 are produced (Everitt et al., 2011). We used a distortion curve to choose the optimum number c of

217 clusters (Sugar et al., 1999), since it shows the evolution of within-cluster sum of squares for

218 increasing number of clusters. Thereafter, we used function *hclust* included in package *fastcluster* for

219 HCA (Müllner, 2013), applied the agglomerative procedure included in the function and divided the

220 data into the required optimum number c of clusters (FSTs).

221 *2.2.2. Classification and Regression Tree (CART) Analysis*

222 After obtaining the HCA results and defining the FSTs that can be identified, we were interested to

223 find out empirical threshold values for the chosen forest attributes ($QMD, GC, BALM$ and N) that can

224 be used to separate different FSTs. To answer this question, we used CART analysis which is a

225 commonly used statistical modelling to identify important ecological patterns (Breiman et al., 1984).

226 For the CART analysis, we employed the package recursive partitioning and regression trees (*rpart*;

227 Breiman et al., 1984), where the HCA results (clusters) were the response variable and

228 $QMD, GC, BALM$ and N the explanatory variables. The QMD and N were log-normalized to avoid

229 the high skewness of their distributions and make them approximately normal. CART resolved values

230 among the explanatory variables that minimize the unexplained variance in response variable, the

231 HCA clusters in this case, recursively splitting the data into those clusters/FSTs. Since the process is

232 recursive, the result resembles a tree where each split is a node with a classification decision between

233 two branches. A large tree was first produced, which was later pruned back to a desired size using

234 function *prune* included in the package *rpart*, and we made it coincide with the optimal c decided

235 upon at the HCA stage.

236 *2.2.3. Classification of Forest Structural Types from ALS Datasets*

237   Supervised machine learning methods use a set of features to generalize phenomena observed from a

238   sample or describe the relationships among indicators. Examples of these methods include maximum

239   likelihood classification, nearest neighbor imputation, artificial neural networks, random forest,

240   support vector machine and naïve Bayes classifier (see e.g. Hastie et al., 2009). In the case of ALS,

241   metrics that describe the distribution of ALS return heights over the forest plots are used to predict a

242   FST that corresponds to each of them (Valbuena et al., 2016a; Adnan et al., 2017). These ALS metrics

243   are then employed as auxiliary variables to make a prediction throughout the scanned area (Næsset,

244   2002; Maltamo et al., 2006). In this study, kNN method of package *class* (Venables and Ripley, 2002)

245   was used for prediction because of its simplicity and capacity to model complex covariance structures.

246   This method has been successfully employed for predicting stand density, volume and cover types

247   (Franco-Lopez et al., 2001). kNN classification is based on dissimilarity measures that are computed

248   as a statistical distance to a reference sample plot in a feature space (Kilkki and Päivinen, 1987), just

249   like those explained for HCA (Eq. 1). The ALS metrics used in the kNN were the maximum of (Max)

250   of ALS return heights over an area, the L-coefficient of variation (Lcv), L-skewness ($Lske$), and the

251   percentage of all returns above 0.1 m ($Cover$), because of their high correlation with the chosen forest

252   attributes (Lefsky et al., 2005; Valbuena et al., 2017). The Max could be related to QMD because of

253   a strong tree diameter-height relationship (Enquist and Niklas, 2001; Sumida et al., 2013) and $Cover$

254   is useful to characterize the stand density (Lefsky et al., 2005; Görgens et al., 2015). Similarly, Lcv

255   and $Lske$ are related to tree dominance (GC and $BALM$) and can be used to detect tree size inequality

256   and light availability (Valbuena et al., 2017; Moran et al., 2018). Description of these ALS metrics

257   and their related proxy forest characteristics are also described in **Table 2**.

258   **** approximate position of Table 2 ****

259   For accuracy assessment we used a leave-one-out cross-validation, which consisted in eliminating

260   each sample plot from the training data before fitting a separate nearest neighbor model for predicting

261   it. *CrossTable* function of package *gmodels* (Warnes, 2013) was used to elaborate a detailed accuracy

262   assessment of the cross-validated contingency metrics and infer their statistical significance. Bias

263   towards each given FST was assessed as the difference between producer's and user's accuracies.

264   Producer's accuracy for a given FST was calculated as the proportion of the observed field plots for

265   that FST which were correctly classified, whereas its user's accuracy was the proportion of field plots

266   being classified as that FST which were correct (Story and Congalton, 1986). To evaluate the degree

267   of misclassification, we calculated the overall accuracy (OA) and kappa coefficient (κ) included in

268   the package *vcd* (Meyer et al., 2014).

269   **3. Results**

270   *3.1. Classification of Field Data into Homogeneous Clusters*

271   The first step was to determine a statistical optimal number of clusters for the HCA, which was found

272   to be $c = 5$ for both the coniferous and deciduous groups, when the decrease in within-cluster

273   variation stabilized after high decreases along the range $c = $ 1-5. In the next step, we identified the

274   threshold values for each explanatory variable – $QMD, GC, BALM$ and N – using CART. Each node

275   maximized the between-cluster explained variability, and thus their order shows the importance of

276   each variable in determining the FSTs (**Figures 2a-b**). In coniferous forest, the first cluster (having

277   lowest within-group variability) was produced by $GC \geq 0.51$ (**Figure 2a**) and, in deciduous forest, it

278   was produced by $BALM > 0.87$ (**Figure 2b**). This iterative procedure was applied on either sides of

279   the classification trees and at the end, clusters with lowest within-cluster variability were produced.

280   *3.2. Identification of Forest Structural Types*

281   The threshold values obtained from each classification tree (**Figures 2a-b**) were used in the

282   identification of the FSTs, which we assigned after inspecting simultaneously their diameter and basal

283   area-weighted distributions (these are the proportions per diameter class of the total number of stems

284   and basal area, respectively). **Table 3** summarizes the characteristics of each FST, and **Figure 3**

285   shows the scatterplots which were also useful for the identification of relevant FSTs.

286   **** approximate position of Table 3 ****

287   **Figure 2a** shows the classification tree and diameter distribution of each FSTs found in the coniferous

288   forest group. Higher GC values (≥ 0.51) produced a neat segregation of reversed J distributions from

289   single storey and multi-layered types. This first cluster were mature sparse reversed J, commonly

290   called peaked reversed J (FST #1.2) because they are characterized by a peak at the right end of their

291   distribution where very big trees take a large proportion of the total basal area (which is best

292   appreciated from the basal area-weighed distributions in **Figs. 2a-b**) The next node identified young

293   forests by their high density of stems ($N > 1,339$ trees·ha^{-1}), which in this case was a young dense

294   single storey FST (*#2.1*). Then the threshold regarded the distinction of very mature single storey

295   (*#2.3*) identified by a high $QMD > 36.6$ cm. The last node separated mature sparse multi-layered

296   FST (*#3.2*) areas from mature single storey FST (*#2.2*) by $BALM \geq 0.67$.

297   **** approximate position of Figure 2 ****

298   **Figure 2b** shows the classification tree and diameter distribution of each FSTs found in deciduous

299   forest. High values of $BALM$ (> 0.87) separated mature sparse reversed J (*#1.2*). As in the coniferous

300   group, the next node identified young dense single storey (*#2.1*) forests by their high stand density,

301    $N > 1,998$ trees·ha^{-1} in this case. The next node found the threshold value of $GC < 0.55$ to identify

302   mature sparse multi-layered (*#3.2*) areas. Higher values of GC were found for the remaining FSTs,

303   young dense multi-layered (*#3.1*) and young dense reversed J (*#1.1*), the latter identified by their

304   lower $QMD > 24.5$ cm.

305   The scatterplot distribution of all FSTs in the feature space of $QMD, GC, BALM$ and N (**Figure 3**)

306   showed that some FSTs are clearly distinct while others present some degree of overlap. The most

307   relevant relationships were found in the cluster disaggregation observed on the $GC - BALM$ feature

308   space, whereas the more traditional $QMD - N$ comparison can be useful to identify young/dense and

309   mature/sparse sub-types.

310   *** *approximate position of Figure 3* ***

311   **Table 4a-b** describes the statistical properties of each FST, where young dense reversed J FST (*#1.1*)

312   and mature sparse reversed J (*#1.2*) were found to be the most frequent FSTs with 29.3% and 51.7%

313   observations in deciduous and coniferous forests, respectively. **Figure 4** shows the thematic map at

314   the permanent plots in Wytham forest, illustrating the natural spatial distributions of the resulting

315   FSTs.

316   *** *approximate position of Table 4* ***

317   *** *approximate position of Figure 4* ***

318   *3.3. Prediction of Forest Structural Types from ALS Datasets*

319   **Table 5** shows the cross-validated results of the kNN predictions of FSTs from ALS datasets of

320   coniferous forest. Mature sparse reversed J/peaked reversed J (*#1.2*) was accurately predicted. Young

321   dense single storey (*#2.1*) and mature single storey (*#2.2*) were slightly underestimated due to a high

322   confusion with mature sparse multi-layered (*#3.2*), which was in turn slightly overestimated. Very

323   mature single storey (*#2.3*) was also slightly overestimated. The overall accuracy of the classification

324   was OA = 0.73 and $\kappa = 0.64$.

325   *** *approximate position of Table 5* ***

326   The results for kNN classification in deciduous forest are shown in **Table 6**. All reversed J diameter

327   distributions were very accurately estimated, both the young dense (*#1.1*) and mature sparse (*#1.2*)

328   reversed J subtypes. The remaining also obtained unbiased predictions, although with lesser accuracy

329   in the estimation following this order: young dense single storey (*#2.1*) and multi-layered (*#3.1*), and

330 mature sparse multi-layered (*#3.2*) being the least accurately estimated because it was the least

331 frequent FST. The prediction was overall fairly unbiased, with OA = 0.87 and $\kappa = 0.81$.

332 *** approximate position of Table 6 ***

4. Discussion

334 In this article we present a two-tier methodology for forest structure classification. The higher tier

335 consists in using values of GC and $BALM$ to characterize reversed J (exponentially decreasing size

336 distributions), single storey and multi-layered. In a lower tier, QMD and N were used to discriminate

337 young/mature and sparse/dense subtypes for each of those described for the higher tier. These FSTs

338 can provide important ecological information about natural dynamics – competitive (self) thinning,

339 mature thinning, and disturbances – (Coomes and Allen, 2007a), or help in identifying where these

340 dynamics have been artificially modified (Valbuena et al., 2016b). In that same order, they also show

341 a degree in tree community development between those ecosystems following metabolic scaling

342 (Enquist and Niklas, 2001) to those regulated by demographic equilibrium (Muller-Landau et al.,

343 2006). The simplicity of this two-tier approach to FSTs makes it feasible for its adoption across

344 ecoregions.

345 The proposed FST classification method has purposely been designed to allow its general application

346 for FSTs other than those present in the case studies shown hereby. The higher tier was proposed by

347 Valbuena (2015) as a comprehensive bivariate description of forest structure, more meaningful than

348 recovering parameters of diameter distributions (Gove, 2004; Lexerød and Eid, 2006). The addition

349 proposed in this article is to include a lower tier of classification, using QMD and N to attaining a

350 greater span of possibilities with FST subtypes according to the stage of development and density of

351 forests. The Valsain site was designed to cover a wide range of plausible FSTs (Valbuena et al., 2012),

352 some occurring by natural dynamics and others driven by management (Valbuena et al., 2013), while

353 those in Finland are highly managed forests (Valbuena et al., 2014, 2016a). With the inclusion of

354 results from Whytham Woods, we have also extended the empirical evidence previously shown for

conifers. The two-tier method should also be largely independent of the sampling design employed.

Any effects due to changes in plot size, sampling design, minimum dbh, etc., would be unimportant

whenever the field data can be employed as good estimators of the variables in hand:

$QMD, GC, BALM$ and N. The estimation of variables like QMD and N is well studied, and known

unbiased when plots are allocated by simple random sampling. Adnan et al. (2017) showed that the

effects of plot size on GC estimation are negligible for the plot sizes involved in this study. To the

best of our knowledge no studies have tackled with $BALM$ estimators, but similar assumptions may

be presumed as per its relationship to the basal area and QMD (Gove 2004). Moreover, these effects

on variable estimators lessen when propagated toward FST classification, because only values

trespassing thresholds have a practical effect. For the purpose of our study we shall assume that the

plots are good estimators of the population values for these variables, and thus changes in the CART

thresholds among classes due to these effects are only marginal.

We used HCA and CART to identify different FSTs using the four forest variables ($QMD, GC, BALM$

and N). HCA is a widely used unsupervised statistical method to classify a large group of observations

into several clusters according to similarity, dissimilarity or distance among individual observations

(Bien and Tibshirani, 2011). On the other hand, CART is a statistical technique for selecting those

variables and their interactions that are most important in determining an outcome or dependent

variable (Breiman et al., 1984). We also used the kNN method (Venables and Ripley, 2002) to predict

those FSTs obtained from ALS datasets (Kim et al., 2009). All these were applied to data from three

biogeographical regions: Boreal, Mediterranean and Atlantic.

There was an interest in exploring empirical threshold values of the four forest variables

($QMD, GC, BALM$ and N), and we used the CART analysis for this purpose (Breiman et al., 1984).

Figures 2a-b show these threshold values at each node for classifying into FSTs. The first nodes were

based on GC and $BALM$ (Gove, 2004; Lexerod and Eid, 2006; Valbuena, 2015), which indicates the

importance of these two parameters in the disaggregation of the higher tier in FSTs classification

379

(**Figure 3**; $BALM - GC$ feature space). The empirical results yielded values of $GC = 0.51$ and $GC = $

380

0.55 (**Figures 2a-b**), which were both very close to the theoretical value at $GC = 0.5$ envisaged by

381

Valbuena et al. (2012) as a beacon for maximum entropy. Multi-layered FSTs are thus signalled

382

around this value, while values below/above must necessarily denote diameter distributions close to

383

Gaussian/negative exponential, respectively. These values were roughly consistent with previous

384

results obtained by Duduman et al. (2011) and Valbuena et al. (2013). Our results from deciduous

385

forest are also similar to those obtained by Simpson et al. (2017) from the same area, however, they

386

used vertical gap probability (proportion ALS returns at specific heights) for structural classification.

387

On the other hand, there was a lack of previous studies analysing empirical values for $BALM$ at

388

different FSTs (Valbuena, 2015). One very relevant result was the peaked reversed J diameter

389

distributions (*#1.2*) which can be identified by large values of $BALM > 0.87$ (**Figure 2b**). This FST

390

was characterized by two distinctive storeys – one mature and spare trees accompanied by dense

391

young ingrowth in the understorey –. Conversely, low values of $BALM < 0.67$ (**Figure 2a**) may

392

indicate the presence of forest ecosystems with very closed canopies and competitive conditions

393

dominated by mature thinning, hence denoting single storey FSTs. Thus, $BALM$ was chosen by the

394

CART algorithm to separate single storey (with lower $BALM$) and multi-layered (with

395

medium/higher $BALM$) (Gove, 2004).

396

The more traditionally used forest variables, QMD and N, were useful to identify lower-tier sub-

397

types: young/mature and dense/sparse FSTs, respectively (Dodson et al., 2012). CART analysis

398

effectively separated the very mature single storey FST (*#2.3*) in coniferous forest (**Figure 2a**) which

399

contained very mature trees (above 100 years old) from Valsaín forest (Spain) as a result of group

400

shelterwood forest management based on long rotation periods (Valbuena et al., 2013). The statistical

401

properties of these FSTs are given in **Table 4a-b**, wherein, young dense reversed J FST (*#1.1*) and

402

mature sparse reversed J/peaked reversed J (*#1.2*) had the largest number of individual observations

403

404 in deciduous and coniferous forests, respectively. The performance of the clustering analysis can also

405 be appreciated in the scatterplot distribution in the feature space of QMD, GC, $BALM$ and N (**Figure**

406 **3**). The widest separation among FSTs was found in the $GC - BALM$ feature space (Gove, 2004)

407 which showed that the GC and $BALM$ are the best indicators in FSTs classifications, as postulated by

408 Valbuena (2015).

409 ALS is a useful tool for the structural heterogeneity assessment (Zimble et al., 2003; Lefsky et al.,

410 2005; Marvin et al., 2014) and mapping of broad forest areas (Asner and Mascaro, 2014). Our results

411 for predicting FSTs from ALS dataset are shown in **Tables 5 and 6**. Generally, unbiased estimations

412 were found in both groups and the observed errors were mostly between FSTs that were, structurally

413 speaking, close to one-another. The highest confusion was found in misclassifying mature single

414 storey (*#2.2*) as mature sparse multi-layered (*#3.2*). These two classes were the most loosely

415 discriminated ones from the forest variables themselves (**Figure 2a**), and thus it was not surprising

416 that they showed worse results in their ALS prediction. Such narrow differences and

417 misclassifications are less important because classifying a mature single storey (*#2.2*) as mature

418 sparse multi-layered (*#3.2*) would have a lesser impact in terms of forest management and practical

419 decision-making than a misclassification as a young dense reversed J (*#1.1*). We obtained a greater

420 overall accuracy and kappa coefficient in the deciduous forest (0.87 and 0.81) as compared to the

421 coniferous forest (0.73 and 0.64), which can be simply due to the differences in the ALS datasets

422 employed in the coniferous group. These accuracies obtained, however, show that the methodology

423 may reliably be applied to disparate ALS datasets surveyed at diverse ecoregions and forest types.

424 The analysis and classification of forest structural types proposed here is of interest for the

425 conservation and promotion of biodiversity, prevention of natural disasters and other ecosystem

426 services. Therefore, forest and natural area managers, nature conservation bodies, landscape planning

427 and ecotourism stakeholders are among the activities and professionals potentially interested in the

428 application of our methodology. Furthermore, this methodology is well adapted to monitor changes

over space and time, as it is based on remote sensors such as LiDAR, which is nowadays used for great extensions and even for nation-wide area coverage. The approach presented in this article could, thanks to its simplicity, be adopted at many different forest types across all geographical zones. It could thus be beneficial for international efforts for harmonizing national forest inventories, initialized by the COST Action E43 (COST, 2006; McRoberts et al., 2008, 2012). At pan-European level it could, for instance, contribute to further developments in the ICP Forests, which is International Co-operative Programme on Assessment and Monitoring of Air Pollution Effects on Forests (JRC, 2011; Giannetti et al., 2018). More globally, it could assist the development of essential biodiversity variables from ALS (Pereira et al., 2013; Proença et al., 2017), and contribute to the use of remote sensing to inform policy-makers on progress towards sustainable development goals and biodiversity targets (O'Connor et al., 2015; Vihervaara et al., 2017).

5. Conclusions

In this research, we developed a region-independent methodology for forest structural types assessment, and demonstrated its utility by using disparate datasets from three biogeographical regions –Boreal, Mediterranean and Atlantic –. The methodology is a simple two-tier approach, feasible for its adoption across ecoregions. We separated FSTs at coniferous (Boreal plus Mediterranean combined) and deciduous (Atlantic) forests, using four forest variables – QMD, GC, $BALM$ and N – and found empirical threshold values for using them in the identification of different FSTs. We found that the GC and $BALM$ are the most important variables in the identification of a higher tier of FSTs: reversed J, single storey and multi-layered. Furthermore, a lower tier young/mature and sparse/dense sub-types can be further identified using QMD and N. We also used nearest neighbour imputation method and the FSTs identified from field data were predicted from ALS data. In spite of using very disparate ALS surveys, the results yielded reliable FST classification. The simplicity of this approach paves the way toward transnational assessments of FSTs across bioregions.

References.

1. Adnan, S., Maltamo, M., Coomes, D.A. and Valbuena, R., 2017. Effects of plot size, stand density, and scan density on the relationship between airborne laser scanning metrics and the Gini coefficient of tree size inequality. Canadian Journal of Forest Research, 47(12), pp.1590-1602.
2. Asner, G.P. and Mascaro, J., 2014. Mapping tropical forest carbon: Calibrating plot estimates to a simple LiDAR metric. Remote Sensing of Environment, 140, pp.614-624.
3. Bergeron, Y., Leduc, A., Harvey, B.D. and Gauthier, S., 2002. Natural fire regime: a guide for sustainable management of the Canadian boreal forest. Silva fennica, 36(1), pp.81-95.
4. Bien, J. and Tibshirani, R., 2011. Hierarchical clustering with prototypes via minimax linkage. Journal of the American Statistical Association, 106(495), pp.1075-1084.
5. Bollandsås, O.M. and Næsset, E., 2007. Estimating percentile-based diameter distributions in uneven-sized Norway spruce stands using airborne laser scanner data. Scandinavian Journal of Forest Research, 22(1), pp.33-47.
6. Bourdier, T., Cordonnier, T., Kunstler, G., Piedallu, C., Lagarrigues, G. and Courbaud, B., 2016. Tree size inequality reduces forest productivity: an analysis combining inventory data for ten European species and a light competition model. PloS one, 11(3), p.e0151852.
7. Breiman, L., Friedman, J.H., Olshen, R.A. and Stone, C.J., 1984. Classification and regression trees. Monterey, Calif., USA: Wadsworth.
8. Coomes, D.A. and Allen, R.B., 2007a. Effects of size, competition and altitude on tree growth. Journal of Ecology, 95(5), pp.1084-1097.
9. Coomes, D.A. and Allen, R.B., 2007b. Mortality and tree-size distributions in natural mixed-age forests. Journal of Ecology, 95(1), pp.27-40.
10. COST: cooperation in the field of science and technology., 2006. Harmonization of national forest inventories in Europe: techniques for common reporting. COST Action E43. Finnish Forest Research Institute.
11. Curtis, R.O., 1982. A simple index of stand density for Douglas-fir. Forest Science, 28(1), pp.92-94.
12. Dodson, E.K., Ares, A. and Puettmann, K.J., 2012. Early responses to thinning treatments designed to accelerate late successional forest structure in young coniferous stands of western Oregon, USA. Canadian journal of forest research, 42(2), pp.345-355.

492 13. Donato, D.C., Campbell, J.L. and Franklin, J.F., 2012. Multiple successional pathways and
493   precocity in forest development: can some forests be born complex?. Journal of Vegetation
494   Science , 23(3), pp.576-584.
495 14. Duduman, G., 2011. A forest management planning tool to create highly diverse uneven-aged
496   stands. Forestry, 84(3), pp.301-314.
497 15. Echeverría, C., Newton, A.C., Lara, A., Benayas, J.M.R. and Coomes, D.A., 2007. Impacts
498   of forest fragmentation on species composition and forest structure in the temperate landscape
499   of southern Chile. Global Ecology and Biogeography, 16(4), pp.426-439.
500 16. Enquist, B.J. and Niklas, K.J., 2001. Invariant scaling relations across tree-dominated
501   communities. Nature, 410(6829), p.655.
502 17. European Environmental Agency., 2018. Biogeographical regions.
503   https://www.eea.europa.eu/data-and-maps/data/biogeographical-regions-europe-3 [accessed
504   May 14, 2018].
505 18. Everitt, B.S., Landau, S., Leese, M. and Stahl, D., 2011. Cluster analysis: Wiley series in
506   probability and statistics.
507 19. Fedrigo, M., Newnham, G.J., Coops, N.C., Culvenor, D.S., Bolton, D.K. and Nitschke, C.R.,
508   2018. Predicting temperate forest stand types using only structural profiles from discrete
509   return airborne lidar. ISPRS Journal of Photogrammetry and Remote Sensing, 136, pp.106-
510   119.
511 20. Franco-Lopez, H., Ek, A.R. and Bauer, M.E., 2001. Estimation and mapping of forest stand
512   density, volume, and cover type using the k-nearest neighbors method. Remote sensing of
513   Environment, 77(3), pp.251-274.
514 21. Giannetti, F., Barbati, A., Mancini, L.D., Travaglini, D., Bastrup-Birk, A., Canullo, R.,
515   Nocentini, S. and Chirici, G., 2018. European Forest Types: toward an automated
516   classification. Annals of Forest Science, 75(1), p.6.
517 22. Görgens, E.B., Packalen, P., Da Silva, A.G.P., Alvares, C.A., Campoe, O.C., Stape, J.L. and
518   Rodriguez, L.C.E., 2015. Stand volume models based on stable metrics as from multiple ALS
519   acquisitions in Eucalyptus plantations. Annals of Forest Science, 72(4), pp.489-498.
520 23. Gougeon, F.A., St-Onge, B.A., Wulder, M. and Leckie, D.G., 2001, August. Synergy of
521   airborne laser altimetry and digital videography for individual tree crown delineation. In
522   Proceedings of the 23rd Canadian Symposium on Remote Sensing (pp. 21-24).
523 24. Gove, J.H., 2004. Structural stocking guides: a new look at an old friend. Canadian journal of
524   forest research, 34(5), pp.1044-1056.
525 25. Gove, J.H., Patil, G.P. and Taillie, C., 1995. A mathematical programming model for
526   maintaining structural diversity in uneven-aged forest stands with implications to other
527   formulations. Ecological Modelling, 79(1-3), pp.11-19.
528 26. Hastie, T., Tibshirani, R. and Friedman, J., 2009. Unsupervised learning. In The elements of
529   statistical learning (pp. 485-585). Springer, New York, NY.
530 27. Hyyppä, J., Hyyppä, H., Leckie, D., Gougeon, F., Yu, X. and Maltamo, M., 2008. Review of
531   methods of small-footprint airborne laser scanning for extracting forest inventory data in
532   boreal forests. International Journal of Remote Sensing, 29(5), pp.1339-1366.
533 28. Jaskierniak, D., Lane, P.N., Robinson, A. and Lucieer, A., 2011. Extracting LiDAR indices
534   to characterise multilayered forest structure using mixture distribution functions. Remote
535   Sensing of Environment, 115(2), pp.573-585.
536 29. JRC: joint research centre., 2011. Biosoil biodiversity executive report. Report number: Joint
537   Research Centre report 64509. Durrant, T., San-Miguel-Ayanz, J., Schulte, E. and Suarez-
538   Meyer, A. (Eds). Publications Office of the European Union. ISSN1018–5593.
539 30. Kilkki, P. and Päivinen, R., 1987. Reference sample plots to combine field measurements and
540   satellite data in forest inventory. Department of Forest Mensuration and Management,
541   University of Helsinki, Research Notes, 19, pp.210-215.

542 31. Kim, S., McGaughey, R.J., Andersen, H.E. and Schreuder, G., 2009. Tree species
543   differentiation using intensity data derived from leaf-on and leaf-off airborne laser scanner
544   data. Remote Sensing of Environment, 113(8), pp.1575-1586.
545 32. Lawrence, R.L. and Wright, A., 2001. Rule-based classification systems using classification
546   and regression tree (CART) analysis. Photogrammetric engineering and remote sensing,
547   67(10), pp.1137-1142.
548 33. Lefsky, M.A., Hudak, A.T., Cohen, W.B. and Acker, S.A., 2005. Geographic variability in
549   lidar predictions of forest stand structure in the Pacific Northwest. Remote Sensing of
550   Environment, 95(4), pp.532-548.
551 34. Lexerød, N. and Eid, T., 2006. An evaluation of different diameter diversity indices based on
552   criteria related to forest management planning. Forest Ecology and Management, 222(1-3),
553   pp.17-28.
554 35. Linder, P., Elfving, B. and Zackrisson, O., 1997. Stand structure and successional trends in
555   virgin boreal forest reserves in Sweden. Forest Ecology and Management, 98(1), pp.17-33.
556 36. Maltamo, M., Bollandsås, O., Næsset, E., Gobakken, T., and Packalén, P. 2010. Different plot
557   selection strategies for field training data in ALS-assisted forest inventory. Forestry, 84(1),
558   pp.23-31.
559 37. Maltamo, M., Eerikäinen, K., Packalén, P. and Hyyppä, J., 2006. Estimation of stem volume
560   using laser scanning-based canopy height metrics. Forestry, 79(2), pp.217-229.
561 38. Maltamo, M., Eerikäinen, K., Pitkänen, J., Hyyppä, J. and Vehmas, M., 2004. Estimation of
562   timber volume and stem density based on scanning laser altimetry and expected tree size
563   distribution functions. Remote Sensing of Environment, 90(3), pp.319-330.
564 39. Maltamo, M., Mehtätalo, L., Vauhkonen, J. and Packalén, P., 2012. Predicting and calibrating
565   tree size and quality attributes by means of airborne laser scanning and field measurements.
566   Canadian Journal of Forest Research, 42(11), pp.1896-1907.
567 40. Maltamo, M., Packalén, P., Yu, X., Eerikäinen, K., Hyyppä, J. and Pitkänen, J., 2005.
568   Identifying and quantifying structural characteristics of heterogeneous boreal forests using
569   laser scanner data. Forest ecology and management, 216(1-3), pp.41-50.
570 41. Marvin, D.C., Asner, G.P., Knapp, D.E., Anderson, C.B., Martin, R.E., Sinca, F. and
571   Tupayachi, R., 2014. Amazonian landscapes and the bias in field studies of forest structure
572   and biomass. Proceedings of the National Academy of Sciences, 111(48), pp.E5224-E5232.
573 42. McElhinny, C., Gibbons, P., Brack, C. and Bauhus, J., 2005. Forest and woodland stand
574   structural complexity: its definition and measurement. McElhinny, C., Gibbons, P., Brack, C.
575   and Bauhus, J., 2005. Forest and woodland stand structural complexity: its definition and
576   measurement. Forest Ecology and Management, 218(1-3), pp.1-24.
577 43. McRoberts, R.E., Winter, S., Chirici, G., Hauk, E., Pelz, D.R., Moser, W.K. and Hatfield,
578   M.A., 2008. Large-scale spatial patterns of forest structural diversity. Canadian Journal of
579   Forest Research, 38(3), pp.429-438.
580 44. McRoberts, R.E., Winter, S., Chirici, G. and LaPoint, E., 2012. Assessing forest naturalness.
581   Forest Science, 58(3), pp.294-309.
582 45. Means, J.E., Acker, S.A., Fitt, B.J., Renslow, M., Emerson, L. and Hendrix, C.J., 2000.
583   Predicting forest stand characteristics with airborne scanning lidar. Photogrammetric
584   Engineering and Remote Sensing, 66(11), pp.1367-1372.
585 46. Meyer, D., Zeileis, A. and Hornik, K., 2014. vcd: Visualizing Categorical Data. R package
586   version 1.3-2.
587 47. Moran, C.J., Rowell, E.M. and Seielstad. C.A., 2018. A data-driven framework to identify
588   and compare forest structure classes using lidar. Remote Sensing of Environment, 211, pp.
589   13-166.
590 48. Moss, I., 2012. Stand structure classification, succession, and mapping using
591   LiDAR (Doctoral dissertation, University of British Columbia).

49. Muller-Landau, H.C., Condit, R.S., Harms, K.E., Marks, C.O., Thomas, S.C., Bunyavejchewin, S., Chuyong, G., Co, L., Davies, S., Foster, R. and Gunatilleke, S., 2006. Comparing tropical forest tree size distributions with the predictions of metabolic ecology and equilibrium models. Ecology Letters, 9(5), pp.589-602.

50. Müllner, D., 2013. fastcluster: Fast hierarchical, agglomerative clustering routines for R and Python. Journal of Statistical Software, 53(9), pp.1-18.

51. Næsset, E., 2002. Predicting forest stand characteristics with airborne scanning laser using a practical two-stage procedure and field data. Remote sensing of environment, 80(1), pp.88-99.

52. Newton, P., 1997. Stand density management diagrams: review of their development and utility in stand-level management planning. Forest Ecology and Management, 98(3), pp.251-265.

53. O'Connor, B., Secades, C., Penner, J., Sonnenschein, R., Skidmore, A., Burgess, N.D. and Hutton, J.M., 2015. Earth observation as a tool for tracking progress towards the Aichi Biodiversity Targets. Remote sensing in ecology and conservation, 1(1), pp.19-28.

54. O'Hara, K.L. and Gersonde, R.F., 2004. Stocking control concepts in uneven-aged silviculture. Forestry, 77(2), pp.131-143.

55. Pascual, C., García-Abril, A., García-Montero, L.G., Martín-Fernández, S. and Cohen, W.B., 2008. Object-based semi-automatic approach for forest structure characterization using lidar data in heterogeneous Pinus sylvestris stands. Forest Ecology and Management, 255(11), pp.3677-3685.

56. Pereira, H.M., Ferrier, S., Walters, M., Geller, G.N., Jongman, R.H.G., Scholes, R.J., Bruford, M.W., Brummitt, N., Butchart, S.H.M., Cardoso, A.C. and Coops, N.C., 2013. Essential biodiversity variables. Science, 339(6117), pp.277-278.

57. Pommerening, A., 2002. Approaches to quantifying forest structures. Forestry: An International Journal of Forest Research, 75(3), pp.305-324.

58. Proença, V., Martin, L.J., Pereira, H.M., Fernandez, M., McRae, L., Belnap, J., Böhm, M., Brummitt, N., García-Moreno, J., Gregory, R.D. and Honrado, J.P., 2017. Global biodiversity monitoring: from data sources to essential biodiversity variables. Biological Conservation, 213, pp.256-263.

59. R Core Team., 2018. R: a language and environment for statistical computing [online]. R Foundation for Statistical Computing, Vienna, Austria. Available from http://www.R-project.org.

60. Savill, P., Perrins, C., Fisher, N. and Kirby, K. eds., 2011. Wytham Woods: Oxford's ecological laboratory. Oxford University Press.

61. Simpson, J.E., Smith, T.E. and Wooster, M.J., 2017. Assessment of Errors Caused by Forest Vegetation Structure in Airborne LiDAR-Derived DTMs. Remote Sensing, 9(11), p.1101.

62. Story, M. and Congalton, R.G., 1986. Accuracy assessment: a user's perspective. Photogrammetric Engineering and remote sensing, 52(3), pp.397-399.

63. Sumida, A., Miyaura, T. and Torii, H., 2013. Relationships of tree height and diameter at breast height revisited: analyses of stem growth using 20-year data of an even-aged Chamaecyparis obtusa stand. Tree physiology, 33(1), pp.106-118.

64. Sugar, C.A. and James, G.M., 2003. Finding the number of clusters in a dataset: An information-theoretic approach. Journal of the American Statistical Association, 98(463), pp.750-763.

65. Valbuena, R., 2015. Forest structure indicators based on tree size inequality and their relationships to airborne laser scanning. Dissertation Forestales, 1, pp. 55-59.

66. Valbuena, R., Packalén, P., Martín-Fernández, S. and Maltamo, M., 2012. Diversity and equitability ordering profiles applied to study forest structure. Forest Ecology and Management, 276, pp.185-195.

67. Valbuena, R., Packalen, P., Mehtätalo, L., García-Abril, A. and Maltamo, M., 2013. Characterizing forest structural types and shelterwood dynamics from Lorenz-based indicators predicted by airborne laser scanning. Canadian journal of forest research, 43(11), pp.1063-1074.

68. Valbuena, R., Vauhkonen, J., Packalen, P., Pitkänen, J. and Maltamo, M., 2014. Comparison of airborne laser scanning methods for estimating forest structure indicators based on Lorenz curves. ISPRS Journal of Photogrammetry and Remote Sensing, 95, pp.23-33.

69. Valbuena, R., Maltamo, M. and Packalen, P., 2016a. Classification of multilayered forest development classes from low-density national airborne lidar datasets. Forestry: An International Journal of Forest Research, 89(4), pp.392-401.

70. Valbuena, R., Eerikäinen, K., Packalen, P. and Maltamo, M., 2016b. Gini coefficient predictions from airborne lidar remote sensing display the effect of management intensity on forest structure. Ecological indicators, 60, pp.574-585.

71. Valbuena, R., Maltamo, M., Mehtätalo, L. and Packalen, P., 2017. Key structural features of Boreal forests may be detected directly using L-moments from airborne lidar data. Remote Sensing of Environment, 194, pp.437-446.

72. Venables, W. N. and Ripley, B. D., 2002. Modern Applied Statistics with S. Fourth edition. Springer.

73. Vihervaara, P., Mononen, L., Auvinen, A., Virkkala, R., Lü, Y., Pippuri, I., Packalen, P., Valbuena, R. and Valkama, J., 2015. How to integrate remotely sensed data and biodiversity for ecosystem assessments at landscape scale. Landscape ecology, 30(3), pp.501-516.

74. Vihervaara, P., Auvinen, A.P., Mononen, L., Törmä, M., Ahlroth, P., Anttila, S., Böttcher, K., Forsius, M., Heino, J., Heliölä, J. and Koskelainen, M., 2017. How essential biodiversity variables and remote sensing can help national biodiversity monitoring. Global Ecology and Conservation, 10, pp.43-59.

75. Warnes, G., 2013. gmodels: Various R programming tools for model fitting. R package version 2.16.2.

76. Weiner, J., 1985. Size hierarchies in experimental populations of annual plants. Ecology, 66(3), pp.743-752.

77. Zimble, D.A., Evans, D.L., Carlson, G.C., Parker, R.C., Grado, S.C. and Gerard, P.D., 2003. Characterizing vertical forest structure using small-footprint airborne LiDAR. Remote sensing of Environment, 87(2-3), pp.171-182.

684 **Tables**

685 **Table 1**. Summary of study area properties

	Finland				Spain				UK			
Number of Plots	79				37				116			
Parameter	Min	Mean	Max	SD	Min	Mean	Max	SD	Min	Mean	Max	SD
QMD	10.33	16.87	29.26	4.09	14.5	33.13	48.3	12.3	10.23	20.92	46.3	6.06
GC	0.21	0.45	0.81	0.15	0.15	0.43	0.87	0.25	0.33	0.69	0.89	0.1
$BALM$	0.52	0.77	0.95	0.08	0.55	0.72	0.93	0.12	0.58	0.81	0.95	0.06
N	425	1,288	2025	612	167	732	1,918	559	75	1,181	3,500	609

	Global			
Number of Plots	232			
Parameter	Min	Mean	Max	SD
QMD	10.23	21.49	48.3	8.76
GC	0.15	0.57	0.89	0.19
$BALM$	0.52	0.78	0.95	0.09
N	75	1,146	3,500	629

686 QMD: quadratic mean diameter (cm); GC: Gini coefficient; $BALM$: Basal area larger than mean; N:
687 stand density (stems.ha^{-1}); SD: standard deviation.

688 **Table 2**. Description of ALS metrics and their related forest characteristics.

Symbol	Description	Proxy forest characteristic
Max	Maximum height of ALS metrics	Dominant tree height
Lcv	L-coefficient of variation	Tree dominance / Tree size inequality
$Lske$	L-skewness of ALS metrics	Tree dominance / Tree size inequality
$Cover$	Percentage of all returns above 0.1 m	Canopy cover

689

690 **Table 3**. Denomination of FSTs based on the four forest structural variables and their

691 characteristics.

FST#	Denomination	Characteristics
#1.1	Young dense reversed J	High GC, medium/high $BALM$, high N, and low QMD
#1.2	Mature sparse reversed J (Peaked reversed J)	High GC, high $BALM$, medium/low N and high QMD
#2.1	Young dense single storey	Medium GC, medium $BALM$, high N and low QMD
#2.2	Mature single storey	Low GC, low $BALM$, medium N and medium QMD
#2.3	Very mature single storey	Low GC, medium/low $BALM$, low N and high QMD
#3.1	Young dense multi-layered	Medium GC, medium $BALM$, low N and high QMD
#3.2	Mature sparse multi-layered	Medium GC, medium $BALM$, medium N and medium QMD

692 QMD: quadratic mean diameter (cm); GC: Gini coefficient; $BALM$: Basal area larger than mean; N:
693 stand density (stems.ha^{-1});

694

695 **Table 4a**. Total number of observations (field plots) and statistical properties of each forest
696 structural type in coniferous group.

Forest Structural Types (FST)		*#1.1*	*#2.1*	*#2.2*	*#2.3*	*#3.2*
Number of Observations		34	22	11	19	30
QMD	Min	11.62	10.33	16.22	36.97	13.22
	Max	22.86	18.81	32.02	48.3	33.86
	Mean	16.60	13.60	23.72	44.14	19.86
	SD	3.20	1.98	4.98	3.08	4.43
GC	Min	0.52	0.27	0.21	0.15	0.22
	Max	0.86	0.5	0.43	0.47	0.5
	Mean	0.68	0.41	0.28	0.25	0.38
	SD	0.10	0.07	0.08	0.10	0.08
$BALM$	Min	0.67	0.64	0.52	0.54	0.67
	Max	0.95	0.85	0.65	0.89	0.87
	Mean	0.84	0.73	0.60	0.66	0.78
	SD	0.07	0.04	0.04	0.09	0.06
N	Min	676	1,375	425-1	167	310
	Max	2200	3025	1146	421	1185
	Mean	1,402	2,000	682	293	805
	SD	383	403	257	74	229

697 QMD: quadratic mean diameter (cm); GC: Gini coefficient; $BALM$: basal areal larger than mean; N:
698 stand density (stems.ha^{-1}); SD: standard deviation.
699 *#1.2:* mature sparse reversed J/peaked reversed J; *#2.1*: young dense single storey; *#2.2*: mature single
700 storey; *#2.3*: very mature single storey; *#3.2*: mature sparse multi-layered.
701
702
703
704
705
706
707
708
709

710
711
712
713
714
715
716
717 **Table 4b**. Total number of observations (field plots) and statistical properties of each forest
718 structural type in deciduous group.

Forest Structural Types (FST)		#1.1	#1.2	#2.1	#3.1	#3.2
Number of Observations		60	22	9	19	6
QMD	Min	12.2	17.96	11.93	24.95	17.00
	Max	24.17	51.27	16.89	62.46	45.70
	Mean	18.52	26.81	13.80	30.50	25.60
	SD	3.02	8.19	1.54	8.09	10.88
GC	Min	0.56	0.64	0.48	0.60	0.40
	Max	0.86	0.91	0.78	0.85	0.54
	Mean	0.71	0.80	0.65	0.72	0.49
	SD	0.08	0.09	0.12	0.08	0.06
$BALM$	Min	0.64	0.87	0.70	0.63	0.69
	Max	0.87	0.99	0.85	0.87	0.83
	Mean	0.80	0.91	0.76	0.80	0.76
	SD	0.05	0.03	0.05	0.07	0.05
N	Min	275	175	2,150	150	300
	Max	1.975	1600	3050	1150	1250
	Mean	1,181	699	2,494	598	871
	SD	389	332	350	246	363

719 QMD: quadratic mean diameter (cm); GC: Gini coefficient; $BALM$: basal areal larger than mean; N:
720 stand density (stems.ha^{-1}); SD: standard deviation.

721   *#1.1*: young dense reversed J; *#1.2*: Mature sparse reversed J (Peaked reversed J); *#2.1*: young
722   dense single storey; *#3.1*: young dense multi-layered; *#3.2*: mature sparse multi-layered.

Table 5. Nearest Neighbour imputation contingency table (coniferous forest: Boreal / Kiihtelysvaara Forest, Finland and Mediterranean / Valsaín Forest, Spain). User's and producer's accuracies are calculated over row and column totals, respectively.

	Observed					
Predicted	*#1.2*	*#2.1*	*#2.2*	*#2.3*	*#3.2*	User's Accuracy
#1.2	26	7	0	0	1	0.76
#2.1	4	11	0	0	1	0.69
#2.2	0	0	3	0	3	0.50
#2.3	4	0	0	19	0	0.83
#3.2	0	4	8	0	25	0.68
Producer's Accuracy	0.76	0.50	0.27	1.00	0.83	

#1.2: mature sparse reversed J/peaked reversed J; *#2.1*: young dense single storey; *#2.2*: mature single storey; *#2.3*: very mature single storey; *#3.2*: mature sparse multi-layered.

Table 6. Nearest Neighbour imputation contingency table (deciduous forest: Atlantic biogeographic region / Wytham woods, UK). User's and producer's accuracies are calculated over row and column totals, respectively.

	Observed					
Predicted	*#1.1*	*#1.2*	*#2.1*	*#3.1*	*#3.2*	User's Accuracy
#1.1	40	0	2	1	0	0.93
#1.2	0	41	0	2	2	0.91
#2.1	0	0	5	1	0	0.83
#3.1	1	1	0	10	2	0.71
#3.2	0	1	0	2	5	0.62
Producer's Accuracy	0.98	0.95	0.71	0.62	0.56	

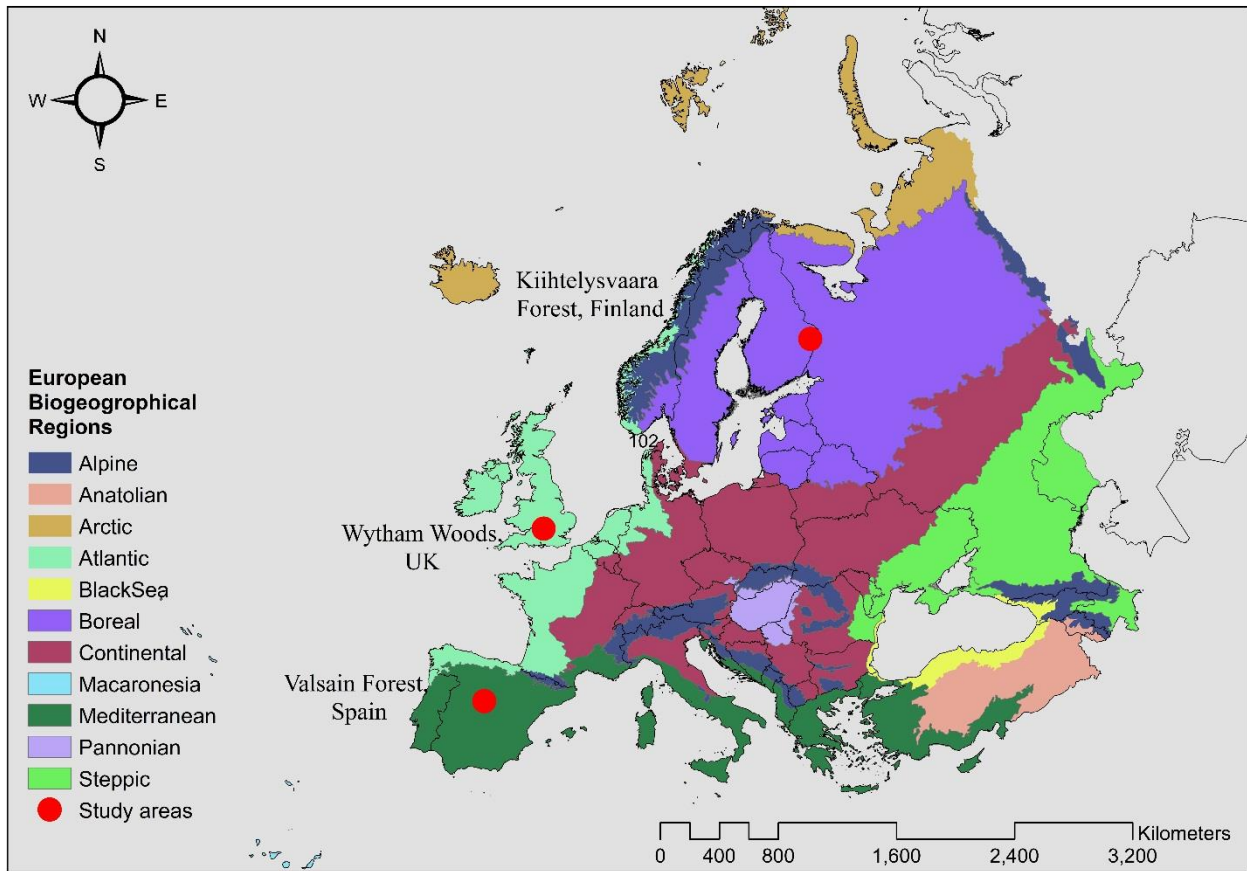*#1.1*: young dense reversed J; *#1.2*: mature sparse reversed J (peaked reversed J); *#2.1*: young dense single storey; *#3.1*: young dense multi-layered; *#3.2*: mature sparse multi-layered.
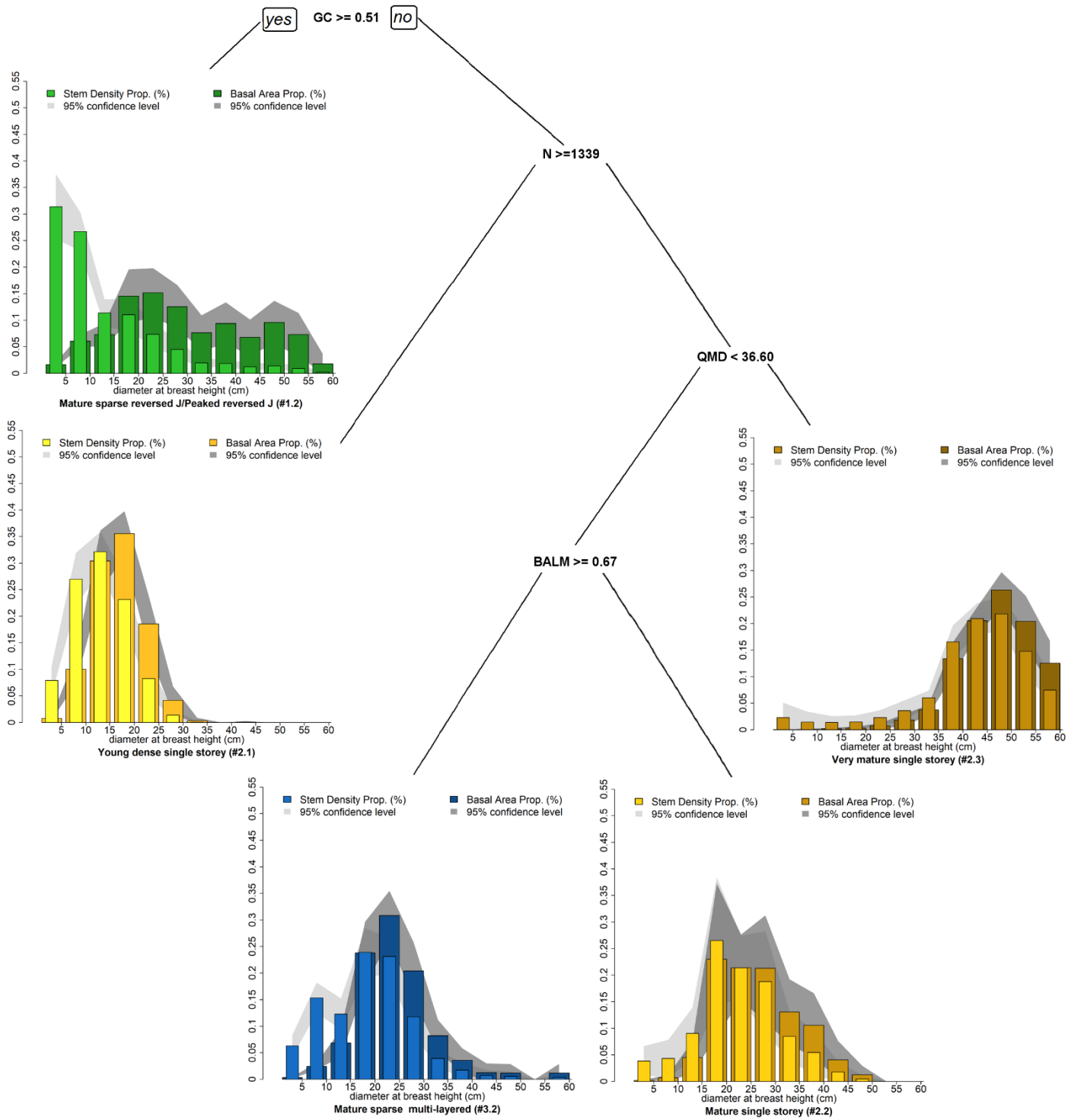
Figure Captions

Figure 1. Map of the European biogeographical regions and the study sites (Boreal/Finland,

Mediterranean/Spain and Atlantic/UK). (European Environmental Agency, 2018)

746   (a)

GC >= 0.51

N >=1339

QMD < 36.60

BALM >= 0.67

Stem Density Prop. (%)   Basal Area Prop. (%)
95% confidence level   95% confidence level

Mature sparse reversed J/Peaked reversed J (#1.2)

diameter at breast height (cm)

Stem Density Prop. (%)   Basal Area Prop. (%)
95% confidence level   95% confidence level

Young dense single storey (#2.1)

diameter at breast height (cm)

Stem Density Prop. (%)   Basal Area Prop. (%)
95% confidence level   95% confidence level

Very mature single storey (#2.3)

diameter at breast height (cm)

Stem Density Prop. (%)   Basal Area Prop. (%)
95% confidence level   95% confidence level

Mature sparse multi-layered (#3.2)

diameter at breast height (cm)

Stem Density Prop. (%)   Basal Area Prop. (%)
95% confidence level   95% confidence level

Mature single storey (#2.2)

diameter at breast height (cm)

747

32

748   (b)

BALM < 0.87   yes   no

N < 1998

GC >= 0.55

QMD < 24.5

Stem Density Prop. (%)   Basal Area Prop. (%)
95% confidence level   95% confidence level
diameter at breast height (cm)
Mature sparse reversed J/Peaked reversed J (#1.2)

Stem Density Prop. (%)   Basal Area Prop. (%)
95% confidence level   95% confidence level
diameter at breast height (cm)
Mature sparse multi-layered (#3.2)

Stem Density Prop. (%)   Basal Area Prop. (%)
95% confidence level   95% confidence level
diameter at breast height (cm)
Young dense single storey (#2.1)

Stem Density Prop. (%)   Basal Area Prop. (%)
95% confidence level   95% confidence level
diameter at breast height (cm)
Young dense reversed J (#1.1)

Stem Density Prop. (%)   Basal Area Prop. (%)
95% confidence level   95% confidence level
diameter at breast height (cm)
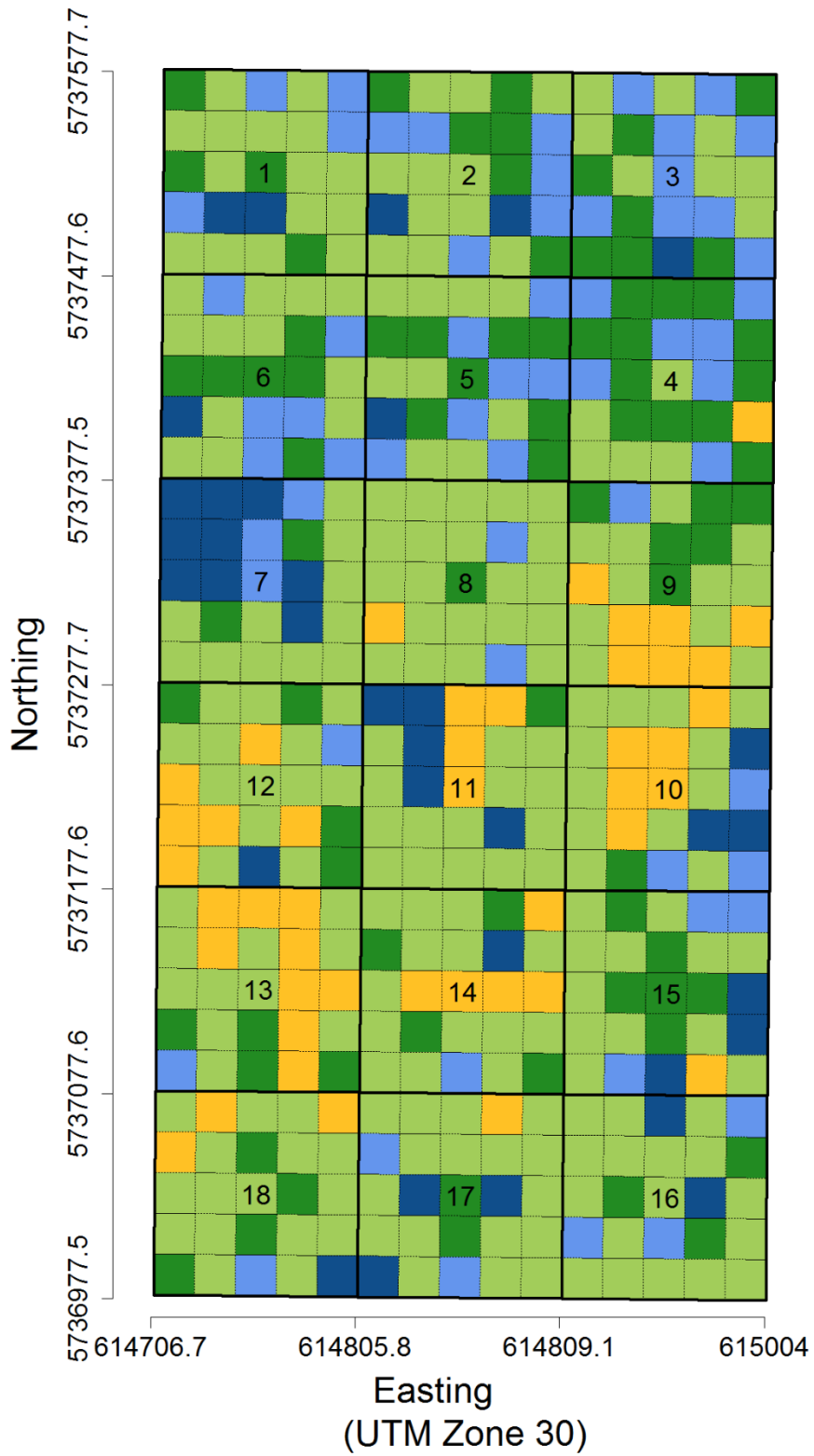Young dense multi-layered (#3.1)

749

33

750 **Figure 2.** Classification tree based on the field data from (a) coniferous forest and (b) deciduous

751 forest as a result classification and regression tree (CART) analysis. Threshold values of the

752 explanatory variables recursively divide the data into homogeneous clusters at each node, according

753 to whether they meet the criterion (positive to the left and negative to the right). Each cluster is then

754 classified as a forest structural type (FST) according to criteria in **Table 3** and their diameter

755 distributions (stem density and basal area proportions, and their 95% confidence intervals are shown).

756 QMD: quadratic mean diameter (cm); GC: Gini coefficient; $BALM$: basal areal larger than mean; and

757 N: stand density (stems.ha^{-1}).
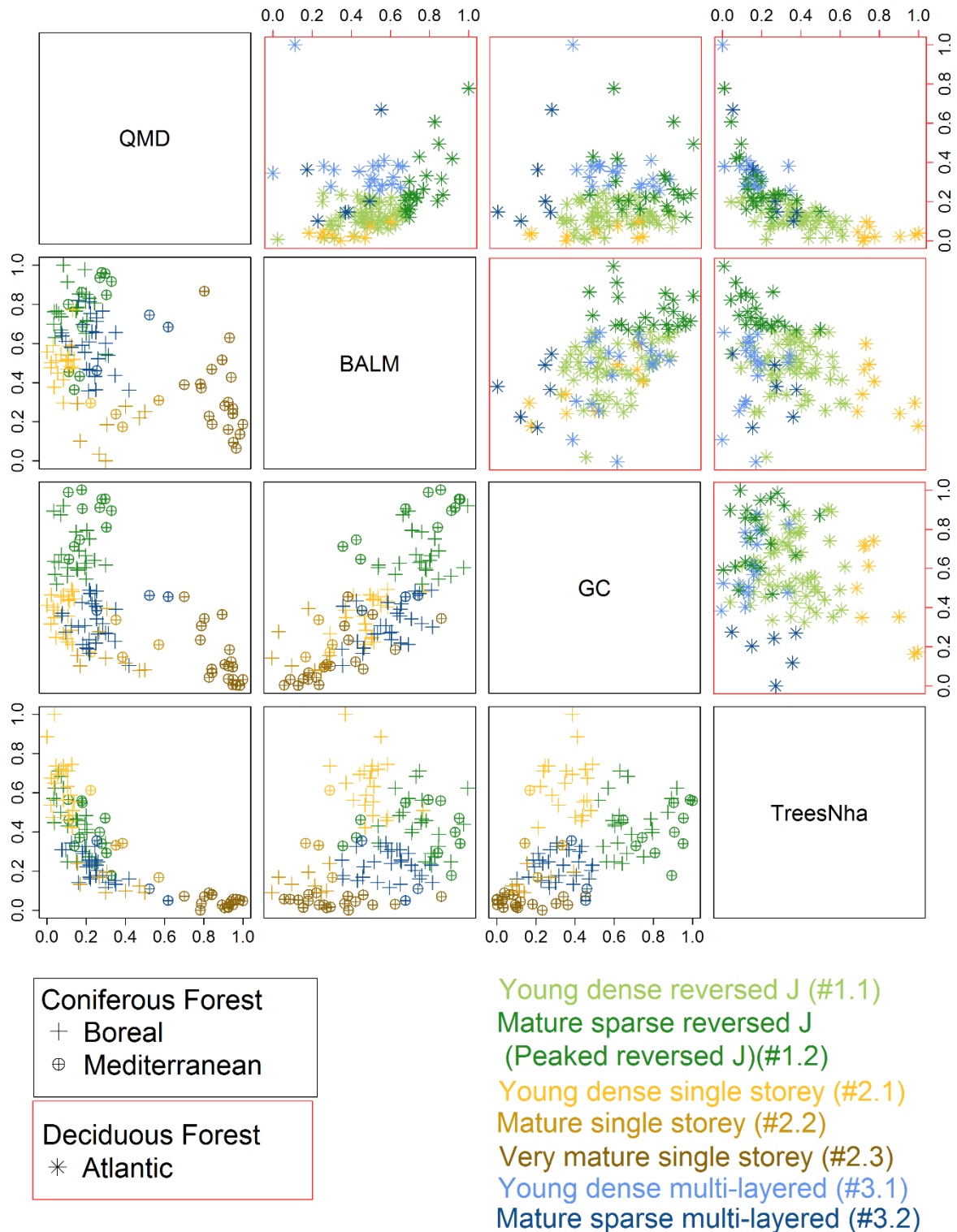
Figure 3. Scatterplot showing five clusters/FSTs in each coniferous and deciduous forest. Axes show the normalized variable values (Eq. 2). (QMD: quadratic mean diameter (cm); $BALM$: Basal area larger QMD; GC: Gini coefficient; N: stand density (stems.ha^{-1}))

758

759

760

761

Easting
(UTM Zone 30)

Young dense reversed J (#1.1)
Mature sparse reversed J/
 Peaked reversed J (#1.2)
Young dense single storey (#2.1)
Young dense multi-layered (#3.1)
Mature sparse multi-layered (#3.2)

763   **Figure 4**. Thematic map showing the natural spatial distribution of the forest structural types based

764   on classification tree and field data from deciduous forest (Atlantic biogeographical region) at

765   Wytham Woods (UK) permanent experimental plots.